

Published in final edited form as:

J Immunol. 2008 August 15; 181(4): 2513–2521.

PD-L1 Regulates a Critical Checkpoint for Autoimmune Myocarditis and Pneumonitis in MRL mice¹

Julie A. Lucas^{*}, Julia Menke^{*}, Whitney A. Rabacal^{*}, Frederick J. Schoen[†], Arlene H. Sharpe[†], and Vicki R. Kelley^{*,2}

^{*} *Laboratory of Molecular Autoimmune Disease, Renal Division, Brigham and Women's Hospital, Boston, MA, 02115, USA*

[†] *Department of Pathology, Harvard Medical School, Brigham and Women's Hospital, Boston, MA, 02115, USA*

Abstract

MRL/MpJ-*Fas^{lpr}* (MRL-*Fas^{lpr}*) mice develop a spontaneous T cell and macrophage (M ϕ) dependent autoimmune disease that shares features with human lupus. Interactions via the PD-1/PD-L1 pathway down-regulate immune responses and provide a negative regulatory checkpoint in mediating tolerance and autoimmune disease. Therefore, we tested the hypothesis that the PD-1/PD-L1 pathway suppresses lupus nephritis and the systemic illness in MRL-*Fas^{lpr}* mice. For this purpose, we compared kidney and systemic illness (lymph nodes, spleen, skin, lung, glands) in PD-L1 null (-/-) and PD-L1 intact (wild-type, WT) MRL-*Fas^{lpr}* mice. Unexpectedly, PD-L1^{-/-};MRL-*Fas^{lpr}* mice died as a result of autoimmune myocarditis and pneumonitis prior to developing renal disease or the systemic illness. Dense infiltrates, consisting of M ϕ and T cells (CD8⁺ > CD4⁺), were prominent throughout the heart (atria and ventricles) and localized specifically around vessels in the lung. In addition, once disease was evident, we detected heart specific autoantibodies (autoAbs) in PD-L1^{-/-};MRL-*Fas^{lpr}* mice. This unique phenotype is dependent on MRL-specific background genes as PD-L1^{-/-};MRL^{+/+} mice lacking the *Fas-lpr* mutation developed autoimmune myocarditis and pneumonitis. Notably, the transfer of PD-L1^{-/-};MRL^{+/+} bone marrow (BM) cells induced myocarditis and pneumonitis in WT;MRL^{+/+} mice, in spite of a dramatic up-regulation of PD-L1 expression on endothelial cells in the heart and lung of WT;MRL^{+/+} mice. Taken together, we suggest that PD-L1 expression is central to autoimmune heart and lung disease in lupus-susceptible (MRL) mice.

Keywords

Rodent; Autoimmunity; Co-stimulation; Knockout Mice; Macrophages

Introduction

Lupus is a human autoimmune disease characterized by chronic inflammation of multiple tissues including kidney, skin, heart, joints, lung, salivary/lacrimal glands and brain. Lesions in MRL-*Fas^{lpr}* mice share many features with those of human lupus (1-3). They develop

¹This work was supported in part by grants from the NIH, R01 DK 52369 (VRK) and PO1 AI 56299 (AHS), and Genzyme Renal Innovations Program (VRK). J. Lucas is supported by a Ruth L. Kirschstein National Research Service Award (F32 DK078416-01). J. Menke received support from the Deutsche Forschungsgemeinschaft (ME-3194/1-1).

² Address correspondence to: Vicki Rubin Kelley, Harvard Institutes of Medicine, 77 Avenue Louis Pasteur, Boston, Massachusetts 02115, USA. Phone: (617) 525–5915; Fax: (617) 525–5830; E-mail: vkelly@rics.bwh.harvard.edu..

disease in the same tissues as humans with lupus, with the notable exception of the heart, and succumb to a fatal kidney disease (50% mortality at 5 mo of age) (4). T cells accumulate in the peripheral lymphoid tissues of MRL-*Fas^{lpr}* mice leading to lymphadenopathy and splenomegaly as a result of a spontaneous mutation in Fas (5,6). These T cells along with M ϕ infiltrate inflamed tissues and are required for disease (7-10). While there are high levels of circulating autoAbs, their role in this disease is unclear (11). Congenic Fas-intact MRL mice (MRL-+/+) develop a latent, less-fulminant lupus (1,12) indicating that background genes are central to lupus in MRL mice (13,14). Since disease is spontaneous and highly predictable in MRL mice, this model is a powerful tool for dissecting the pathogenesis of lupus.

The B7/CD28 co-stimulatory pathway regulates immune cell activation. We previously reported that B7.1 and B7.2 expression promotes lupus since B7.1/B7.2 null MRL-*Fas^{lpr}* mice are protected from renal disease and the systemic illness (15). Recent attention has focused on an additional member of this family of co-stimulatory molecules, PD-1 and its ligands PD-L1 and PD-L2. PD-1, is broadly expressed on multiple hematopoietic cells including: T cells, B cells, monocytes, and M ϕ , upon activation (16-18). Similarly, PD-L1, is expressed by a variety of cell types, including APCs and a broad range of parenchymal cells (19). For the most part, engagement of PD-1 inhibits T and B cell functions (20). PD-1 and PD-L1 are integral in suppressing autoimmune kidney disease. In particular, PD-1 null mice on the C57BL/6 (B6) background (PD-1^{-/-};B6) develop mild, focal glomerulonephritis, which increases in incidence and severity in mice with the *Fas^{lpr}* mutation (PD-1^{-/-};B6-*Fas^{lpr}*) (21). However, the pathology in the renal interstitium, tubules, and vasculature, as well as the mechanisms responsible for inciting glomerular disease was not explored. Furthermore, kidney pathology and function was exacerbated in PD-L1^{-/-};B6 mice during induced autoimmune kidney disease, nephrotoxic serum nephritis (17). Thus, the PD-1/PD-L1 pathway dampens autoimmune responses in the kidney.

Our goal was to test the hypothesis that elimination of PD-1/PD-L1 signaling exacerbates MRL-*Fas^{lpr}* lupus nephritis and the systemic illness. For this purpose, we generated PD-L1^{-/-};MRL-*Fas^{lpr}* and PD-L1^{-/-};MRL-+/+ mice. Unexpectedly, PD-L1^{-/-};MRL-*Fas^{lpr}* and PD-L1^{-/-};MRL-+/+ mice succumbed to autoimmune myocarditis and pneumonitis prior to the development of lupus nephritis and systemic features characteristic of MRL mice. This suggests the PD-1/PD-L1 pathway is providing an essential negative regulatory checkpoint to prevent autoimmune heart and lung disease in MRL mice.

Materials and Methods

Mice

PD-L1^{-/-} mice on the B6 background (PD-L1^{-/-};B6) were generated previously (22). MRL/MpJ (MRL-+/+) and MRL/MpJ-*Fas^{lpr}*/J (MRL-*Fas^{lpr}*) mice were purchased from The Jackson Laboratories. PD-L1^{-/-};B6 mice were backcrossed to MRL-*Fas^{lpr}* mice for 6 generations (N6). Since the genes for PD-L1 and Fas are both on chromosome 19, we screened large numbers of mice for recombinants. Genotyping for PD-L1 (22) and Fas (23) were performed as previously described. MRL-*Fas^{lpr}* and MRL-+/+ mice will be referred to collectively as MRL mice. PD-L1^{-/-};B6 mice were backcrossed to MRL-+/+ mice for 10 generations (N10). Mice were housed and bred in a pathogen-free animal facility. Use of mice in our study was reviewed and approved by the Standing Committee on Animals in the Harvard Medical School in adherence to the NIH Guide for the care and use of laboratory animals.

Histopathology

Heart, lung, liver, and kidney tissues were fixed overnight in 10% neutral buffered formalin, stored in 70% ethanol, and embedded in paraffin. Sections (4 μ m) were stained with H&E.

Myocarditis—Myocarditis was graded as previously described (24) by microscopic examination of H&E-stained mid-ventricular cross sections using a 0–4 scale as follows: Grade 0) no inflammation; Grade 1) one to five distinct inflammatory foci with total involvement of 5% or less of the cross-sectional area; Grade 2) more than five distinct inflammatory foci, or involvement of >5% but <20% of the cross-sectional area; Grade 3) diffuse inflammation involving over 20–50% of the area; Grade 4) diffuse inflammation involving >50% of the area.

Pneumonitis—Inflammatory lung lesions were graded by microscopic examination of a near-complete H&E stained cross-section of inflated lung using a 0–4 scale as follows: Grade 0) no inflammation; Grade 1) one to two distinct perivascular and/or peribronchial inflammatory foci in the cross-sectional area; Grade 2) three to four lesions; Grade 3) four to eight lesions; Grade 4) more than nine lesions.

Nephritis—We assessed kidney pathology on periodic acid-Schiff's reagent stained sections of PD-L1^{-/-};MRL-Fas^{lpr} and WT;^{MRL-Fas^{lpr}} mice at 2 mo of age as previously described (17).

Blood Urea Nitrogen

We assessed the levels of blood urea nitrogen in serum of PD-L1^{-/-};MRL-Fas^{lpr} and WT;^{MRL-Fas^{lpr}} mice at 2 mo of age as previously described (17).

Immunohistochemistry

Heart and lung tissue was processed and stained for the presence of CD68, CD4, CD8, PD-1, and PD-L1 as previously described for the kidney (17).

PD-1 Expression on Leukocyte Subsets in Heart and Lung

We prepared single cell suspensions from lung tissue by mashing the entire lung between 40 µm nylon cloth mesh (Thermo Fisher Scientific) with a plastic syringe barrel in RPMI-10. Single cell suspensions from the heart were prepared by cutting the heart into pieces (<1 mm) with a razor blade followed by incubation with collagenase type IV (1mg/ml, Worthington Biochemical) in HBSS (Gibco/Invitrogen) supplemented with 5 mM CaCl₂ at 37°C for 45 min. Following digestion, tissue was dissociated by pipetting and the resulting cell solution was filtered through 40 µm mesh to remove undigested tissue. Red blood cells were lysed by incubation in ACK lysis buffer for 5 min at RT. Cells were washed twice with 10 ml RPMI-10 and re-filtered. We stained these cells with fluorescently labeled Abs as previously described (10). We collected heart (5 – 10 × 10⁴) and lung (1 – 2 × 10⁵) cells using a FACS Calibur (Becton Dickinson) and analyzed the data using Flowjo software (Tree Star). We used the following Abs from eBioscience for FACS analysis: FITC-conjugated anti-CD45.1 (A20); PE-conjugated anti-PD-1 (J43), PE-Cy5 conjugated anti-CD8 (53–6.7) and anti-CD11c (N418); and allophycocyanin-conjugated anti-CD4 (L3T4) and anti-CD45.1 (A20). We also used FITC-conjugated CD11b (M1/70) from Pharmingen and FITC-conjugated anti-CD68 (FA11) from Serotec.

Cardiac AutoAb ELISAs

To detect ant-cardiac myosin or anti-cardiac troponin I autoAbs, we coated 96-well plates with porcine cardiac myosin (5 µg/ml, Sigma) or mouse cardiac troponin I (1 µg/ml, Life Diagnostics, Inc) in bicarbonate buffer overnight. After blocking with 1% BSA in PBS, we added diluted serum samples (1:50, 1:200, 1:800, 1:3200, and 1:6400). Bound autoAbs were detected with HRP conjugated anti-mouse IgG, IgG1, IgG2a, and IgG2b Abs (1:1000, Southern Biotechnology Associates), developed with TMB, and stopped with H₂SO₄. Serum from age-matched B6 mice was used as a negative control. Optical densities were measured at 450nm.

Antibody endpoint titers for each mouse were determined as the greatest positive dilution of serum.

dsDNA ELISA

We analyzed the anti-dsDNA autoAb (total IgG) in the sera of PD-L1^{-/-};MRL-Fas^{lpr} and WT;MRL-Fas^{lpr} mice diluted 1:50 as previously reported (25).

C3 Deposits

To determine the optimal concentration of anti-mouse C3 for staining we tested a large range of serial dilutions (1:2000; 1:4000; 1:8000; 1:32,000; 1:64000; 1:128,000; 1:256,000; and 1:512,000). Based on the results, we stained heart and lung sections from PD-L1^{-/-};MRL-Fas^{lpr} and WT;MRL-Fas^{lpr} mice (1 and 2 mo) with fluorescein-conjugated anti-mouse C3 (1:8000, Capell/ICN) for 30 min at RT. Sections were mounted in Vectashield + DAPI (Vector) and analyzed immediately with a fluorescent microscope. The sections were scored based on the area of the cross-section with positive staining: Score 0) no specific staining; Score 0.5) 1–5%; Score 1) 5–10%; Score 2) 11–15%; Score 2.5) 16–20%; Score 3) 20–30%.

Bone Marrow Chimeras

We isolated BM from PD-L1^{-/-};MRL^{+/+} or WT;MRL^{+/+} (PD-L1^{+/+};MRL^{+/+} and PD-L1^{+/-};MRL^{+/+}) mice as previously described (26). PD-L1^{+/-};MRL^{+/+} hosts (1 mo) were lethally irradiated (1000 rads) and reconstituted with PD-L1^{-/-};MRL^{+/+} or WT;MRL^{+/+} BM cells ($5 - 7 \times 10^6$). We monitored BM chimeric mice for signs of illness (labored breathing, lethargy, ect) and sacrificed mice at the onset of symptoms. Control mice were sacrificed on the same day as the last PD-L1^{-/-};MRL^{+/+} BM chimera. We evaluated the transfer of heart and lung disease by histopathology and immunostaining of heart and lung sections.

Statistical Analysis

The data represent the mean \pm SEM and were prepared using Graph-Pad Prism Version 4.0 (Graph Pad, San Diego, CA). We used the non-parametric Mann-Whitney *U* Test to evaluate *p* values.

Results

Survival is reduced in PD-L1^{-/-};MRL-Fas^{lpr} mice

To evaluate the role of the PD-1 pathway in the systemic autoimmune disease in MRL-Fas^{lpr} mice, we generated PD-L1^{-/-};MRL-Fas^{lpr} mice. We tested the hypothesis that autoimmune disease in MRL-Fas^{lpr} would be exacerbated in PD-L1^{-/-};MRL-Fas^{lpr} mice. In fact, PD-L1^{-/-};MRL-Fas^{lpr} mice died much earlier than their PD-L1^{+/-};MRL-Fas^{lpr} and PD-L1^{+/+};MRL-Fas^{lpr} (wild-type, WT;MRL-Fas^{lpr}) littermates (Fig 1A). The increased mortality occurred in both male and female PD-L1^{-/-};MRL-Fas^{lpr} mice with median survival times of 9 and 11 wk, respectively. This is noteworthy since disease is typically delayed in male MRL-Fas^{lpr} mice. In contrast, none of the WT;MRL-Fas^{lpr} mice died prior to 20 wk of age. Thus, survival is dramatically decreased in PD-L1^{-/-};MRL-Fas^{lpr} mice.

PD-L1^{-/-};MRL-Fas^{lpr} mice die as a result of myocarditis-induced heart failure

The phenotypic expression of disease drastically changed in PD-L1^{-/-};MRL-Fas^{lpr} compared to the WT;MRL-Fas^{lpr} mice. Autoimmune disease in WT;MRL-Fas^{lpr} mice is characterized by massive lymphadenopathy, splenomegaly, skin lesions, and fatal renal disease at 5–6 mo of age. In contrast, PD-L1^{-/-};MRL-Fas^{lpr} mice died between 2 and 3 mo of age from congestive heart failure with extensive edema, ascites, pleural effusions, massively enlarged hearts with areas of discoloration (Fig 1B), inflamed lungs, and large congested livers. Of note, with the

exception of an increase in spleen weight, the PD-L1^{-/-};MRL-Fas^{lpr} mice did not share any of the gross characteristic features of moribund MRL-Fas^{lpr} mice (data not shown). Since MRL-Fas^{lpr} mice do not develop myocarditis, these data indicate that PD-L1^{-/-};MRL-Fas^{lpr} mice succumb to a disease that differs from the WT strain resulting in early death.

To more fully explore this novel phenotype, we compared the histopathology of hearts, lungs, livers, and kidneys from moribund PD-L1^{-/-};MRL-Fas^{lpr} and WT;MRL-Fas^{lpr} mice. In hearts, from PD-L1^{-/-};MRL-Fas^{lpr} mice, lesions were characterized by a pancarditis involving the walls of all chambers; they spanned the endocardium, myocardium, and epicardium and the atria and ventricles, bilaterally. The right ventricle was often involved transmurally at a single site and some areas had focal wall thinning. Lesions consisted typically of dense mononuclear infiltrates with associated myocyte injury (Fig 2A, arrowhead) in a patchy to diffuse distribution. In contrast, the hearts of WT;MRL-Fas^{lpr} mice were histologically normal with no evidence of infiltrates (Fig 1B, 2A). PD-L1^{-/-};MRL-Fas^{lpr} lung-lesions typically consisted of focal collections of mononuclear inflammatory cells in a predominantly perivascular (Fig 2B, arrows) but occasionally peribronchial location. Lung lesions were occasionally seen in WT;MRL-Fas^{lpr} mice in the absence of myocardial pathology. Conversely, myocardial lesions without lung pathology was rarely noted in PD-L1^{-/-};MRL-Fas^{lpr} mice. In addition, small perivascular inflammatory lesions were evident in the livers of nearly all PD-L1^{-/-};MRL-Fas^{lpr} mice at the time of death (data not shown). Interestingly, we did not detect an increase in leukocytic infiltrates in the kidneys of PD-L1^{-/-};MRL-Fas^{lpr} mice as compared to age-matched WT;MRL-Fas^{lpr} mice (Fig 2C). And, although we detected a modest increase in glomerular pathology, we did not detect a loss of renal function (blood urea nitrogen) in moribund PD-L1^{-/-};MRL-Fas^{lpr} mice as compared to age-matched WT;MRL-Fas^{lpr} mice (data not shown). Thus, the early demise in PD-L1^{-/-};MRL-Fas^{lpr} mice did not result from an acceleration in renal disease, but rather from fulminant heart and lung pathology.

Inflammation arises in the heart and lung concurrently in PD-L1^{-/-};MRL-Fas^{lpr} mice

To determine the temporal development of myocarditis and pneumonitis in PD-L1^{-/-};MRL-Fas^{lpr} mice, we analyzed heart and lung pathology at multiple time points (2wk, 1, and 2mo) (Fig 2D). There were signs of disease in the heart and lungs of some PD-L1^{-/-};MRL-Fas^{lpr} mice by 2 wk of age and the incidence and severity progressively rose between 1 and 2 mo of age. By comparison, heart disease was not detectable and lung disease was less severe in WT;MRL-Fas^{lpr} mice. Due to the rapidity of disease, it was not possible to determine by morphologic criteria whether disease arose first in the heart or lung of PD-L1^{-/-};MRL-Fas^{lpr} mice. Thus, we conclude myocarditis and pneumonitis arise concurrently in PD-L1^{-/-};MRL-Fas^{lpr} mice.

M ϕ and T cell infiltrates are increased in the heart and lung of PD-L1^{-/-};MRL-Fas^{lpr} mice

To identify the intra-cardiac and intra-pulmonary leukocytes in PD-L1^{-/-};MRL-Fas^{lpr} mice, we examined the accumulation of M ϕ , T (CD4⁺ and CD8⁺), and B220⁺ cells over a 2 month period (Fig 3). We detected more M ϕ than CD8⁺ T cells and very few CD4⁺ T cells in the heart in PD-L1^{-/-};MRL-Fas^{lpr} mice at 2 wks of age. The relative numbers of each of these leukocyte populations progressively increased from 2 wk through 2 mo of age specifically in PD-L1^{-/-};MRL-Fas^{lpr}, while the small number of resident leukocytes in the heart of WT;MRL-Fas^{lpr} mice did not change (Fig 3A). Of note, while dendritic cells express CD68, we determined that the CD68⁺ cells in the heart are primarily M ϕ by flow cytometry, as these cells express high levels of CD11b and are auto-fluorescent (27) (data not shown). Since lymphadenopathy and splenomegaly typical of WT;MRL-Fas^{lpr} mice is predominately comprised of a unique population of CD4⁻CD8⁻ T cells that express the B cell determinant, B220 (double negative (DN) T cells), we also probed for B220⁺ cells. We did not detect an increase in B220⁺ cells in the hearts of PD-L1^{-/-};MRL-Fas^{lpr} as compared to WT;MRL-Fas^{lpr} mice at any time point,

indicating that neither DN T cells or B cells are in the hearts of PD-L1^{-/-};MRL-Faslpr mice during myocarditis. The lack of DN T cell infiltrates in the heart is likely due to the age of the mice at the time of death. The B220⁺ DN T cells that are characteristic of MRL-Faslpr mice do not become abundant until 2 – 3 mo of age. Taken together, these results suggest destruction of myocytes in PD-L1^{-/-};MRL-Faslpr mice is mediated largely by M ϕ , CD8⁺ and/or CD4⁺ T cells.

The lungs, in contrast to the heart, had substantial numbers of resident leukocytes, the majority of which were CD68⁺ alveolar M ϕ and DC, with fewer T and B cells. We detected an increase in interstitial (data not shown) and perivascular (Fig 3B) leukocytes in PD-L1^{-/-};MRL-Faslpr as compared to WT;MRL-Faslpr mice at 2 wk of age. Perivascular infiltrates consisting of M ϕ , T cells, and B220⁺ cells, which were evident at 2 wk of age, progressively increased until 2 mo of age, but were notably absent in WT;MRL-Faslpr mice (Fig 3B). To distinguish whether the B220⁺ cells in the lungs of PD-L1^{-/-};MRL-Faslpr mice were DN T cells or B cells, we stained lung sections for the presence of B cell specific proteins, CD79 (Fig 3B, bottom left panel) and CD19 (data not shown). We determined that the majority of these B220⁺ cells were B cells. As B cells can be inhibitory during autoimmune responses (28), it is intriguing to hypothesize that these B cells may be playing a regulatory role during pneumonitis in PD-L1^{-/-};MRL-Faslpr mice. Regardless, PD-L1 limits the accumulation of B cells, along with M ϕ and T cells (CD4⁺ and CD8⁺) in the lungs of MRL-Faslpr mice.

PD-1 expressing leukocytes increase in the heart and lung of PD-L1^{-/-};MRL-Faslpr mice

To define the leukocytes in the heart and lung in the PD-L1^{-/-};MRL-Faslpr mice with myocarditis and pneumonitis that express PD-1, we evaluated PD-1 expression on infiltrating leukocytes. The vast majority of infiltrating cells in the heart of PD-L1^{-/-};MRL-Faslpr mice with myocarditis expressed PD-1 (Fig 4A, top right panel). In contrast, PD-1 is barely detected in the WT;MRL-Faslpr mice with normal hearts (Fig 4A, top left panel). Similarly, PD-1 expression was drastically up-regulated in the lung of PD-L1^{-/-};MRL-Faslpr mice with pneumonitis and localized primarily to the perivascular leukocytes (Fig 4A, bottom right panel). As in the heart, PD-1 expression was sparse in the lung of WT;MRL-Faslpr mice where it localized to the few perivascular leukocytes (Fig 4, bottom left inset). Using flow cytometry, we determined that PD-1 was expressed on M ϕ and T (CD4⁺ and CD8⁺) cells (Fig 4B), but not B220⁺ cells (data not shown) in the heart and lung of PD-L1^{-/-};MRL-Faslpr mice with myocarditis and pneumonitis. Interestingly, we did not detect an increase in PD-1⁺ cells in the spleen, kidney, or liver of PD-L1^{-/-};MRL-Faslpr mice (data not shown). Thus, PD-1⁺ M ϕ and T cells accumulate specifically in the heart and lung of PD-L1^{-/-};MRL-Faslpr mice during myocarditis and pneumonitis.

PD-L1^{-/-};MRL-Faslpr mice develop anti-cardiac myosin specific autoAbs

Heart-specific autoAbs are common during myocarditis and may contribute to disease (29). As the most abundant antigen in the heart is cardiac myosin (30), we tested whether PD-L1^{-/-};MRL-Faslpr mice generated anti-cardiac myosin autoAbs. We detected high titers of anti-cardiac myosin autoAbs (total IgG) in PD-L1^{-/-};MRL-Faslpr mice (1:5300 \pm 700, n=10) in comparison to minimal levels in WT;MRL-Faslpr mice (1:560 \pm 150, n=6) at 2 mo of age (p<0.01). In particular, we detected an increase in the titers of IgG1 and IgG2a, and to a lesser extent IgG2b, isotypes of anti-cardiac myosin autoAbs (data not shown). Anti-cardiac troponin I autoAbs have been detected in PD-1^{-/-};BALB/c mice and contribute to the development of dilated cardiomyopathy (31). Therefore, we also probed for the presence of anti-cardiac troponin I autoAbs. Likewise, we detected increased titers of anti-cardiac troponin I autoAbs (total IgG) in PD-L1^{-/-};MRL-Faslpr mice (1:733 \pm 67, n=9) in comparison to WT;MRL-Faslpr mice (1:286 \pm 87, n=7) at 2 mo of age (p<0.05). Interestingly, we did not detect anti-cardiac myosin autoAbs (2wks and 1 mo) or anti-cardiac troponin I autoAbs (1 mo) prior to overt

disease. Therefore, we explored the possibility that cardiac-autoAbs deposit in the heart, which prevents detection in the serum prior to overt disease. For this purpose, we measured C3 deposits in the heart of PD-L1^{-/-};MRL-Fas^{lpr} and WT;MRL-Fas^{lpr} mice at 1 and 2 mo of age. While we detected an increase of C3 deposits in PD-L1^{-/-};MRL-Fas^{lpr} as compared to WT;MRL-Fas^{lpr} hearts at 2 mo of age, we did not detect a difference at 1 mo of age (data not shown). This is consistent with the concept that cardiac-specific autoAbs rise once the heart muscle is damaged. Of note, titers of anti-dsDNA autoAbs were not increased in PD-L1^{-/-};MRL-Fas^{lpr} mice as compared to WT;MRL-Fas^{lpr} mice at 2 mo of age. (data not shown). This indicates that the increase cardiac-autoAbs is specific to the unique autoimmune disease in PD-L1^{-/-};MRL-Fas^{lpr} mice, as opposed to a broad increase in autoAb production. In spite of the specificity of these autoAbs, their late emergence contrasts with the early emergence of these autoAbs in PD-L1^{-/-};BALB/c mice (31,32) and suggests that cardiac autoAbs do not initiate disease in PD-L1^{-/-};MRL-Fas^{lpr} mice.

Development of autoimmune myocarditis and pneumonitis in PD-L1^{-/-};MRL mice is not dependent on the Fas^{lpr} mutation

The Fas^{lpr} mutation converts a mild, latent autoimmune disease in MRL^{+/+} mice into a fulminant and severe disease in MRL-Fas^{lpr} mice (2,4). To determine whether the Fas^{lpr} mutation is required for the autoimmune myocarditis and pneumonitis in PD-L1^{-/-};MRL-Fas^{lpr} mice, we generated PD-L1^{-/-};MRL^{+/+} mice. Similar to PD-L1^{-/-};MRL-Fas^{lpr} mice, PD-L1^{-/-};MRL^{+/+} mice die at a young age. Remarkably, the median survival time of PD-L1^{-/-};MRL^{+/+} mice (male and female) was 5 wk (Fig 5A). In contrast, the average life-span of WT;MRL^{+/+} mice ranges from one and two years of life (Jackson Laboratories strain 000486 information). In addition, PD-L1^{-/-};MRL^{+/+} mice develop myocarditis and pneumonitis (Fig 5B, C) similar to PD-L1^{-/-};MRL-Fas^{lpr} mice (Fig 2). The pattern of anti-cardiac myosin and anti-cardiac troponin I autoAbs in PD-L1^{-/-};MRL^{+/+} mice was similar in quantity and isotype expression to PD-L1^{-/-};MRL-Fas^{lpr} mice (data not shown). Thus, autoimmune myocarditis and pneumonitis is dependent on the MRL background and not on the Fas^{lpr} mutation in PD-L1^{-/-};MRL-Fas^{lpr} mice.

PD-L1^{-/-};MRL^{+/+} hematopoietic BM cells are sufficient to induce autoimmune myocarditis and pneumonitis in WT;MRL^{+/+} chimeras

PD-L1 is widely expressed on hematopoietic and parenchymal cells in many tissues (19). To determine whether PD-L1^{-/-};MRL^{+/+} hematopoietic cells are sufficient to confer disease, we transferred PD-L1^{-/-};MRL^{+/+} or WT;MRL^{+/+} BM into lethally irradiated WT;MRL^{+/+} mice (Fig 6). The WT;MRL^{+/+} recipients of PD-L1^{-/-};MRL^{+/+} BM developed signs of disease (lethargy, labored breathing, swollen belly) following reconstitution (4–6wk). We detected myocarditis and pneumonitis rich in CD68⁺, CD8⁺, and CD4⁺ leukocytes (Fig. 6, left panels) in WT;MRL^{+/+} recipients of PD-L1^{-/-};MRL^{+/+} BM, but not of WT;MRL^{+/+} BM (Fig 6, right panels). We also transferred PD-L1^{-/-};MRL^{+/+} BM into irradiated PD-L1^{-/-};MRL^{+/+} mice (4wk) and found that these mice developed myocarditis and pneumonitis by 2 wk post-transfer (data not shown). Since the life-span of these mice was similar to unmanipulated PD-L1^{-/-};MRL^{+/+} mice (5–6 wks), we can not distinguish between the disease that may have been present at the initiation of the experiment and disease induced by the transfer of PD-L1^{-/-};MRL^{+/+} BM. However, it is clear that PD-L1^{-/-};MRL^{+/+} hematopoietic BM cells are sufficient to induce myocarditis and pneumonitis in WT;MRL^{+/+} mice.

PD-L1 is up-regulated on parenchymal cells in the heart and lung when inflammation is induced in WT;MRL^{+/+} mice

Although PD-L1^{-/-} hematopoietic cells are sufficient to induce myocarditis and pneumonitis in WT;MRL^{+/+} BM chimeras, disease is less severe than in PD-L1^{-/-};MRL^{+/+} mice, as

determined by histopathological criteria (data not shown). The delayed tempo of disease in these chimeras suggests that PD-L1 expression on parenchymal cells in WT;^{MRL-+/+} BM chimeras may limit disease. To investigate this possibility, we evaluated PD-L1 expression in the heart and lung of WT;^{MRL-+/+} BM chimeras (Fig 7). PD-L1 expression was robust in the heart and lung of PD-L1^{-/-};^{MRL-+/+} BM recipients (Fig 7, top left panel), but not in WT;^{MRL-+/+} BM recipients (Fig 7, top middle panel). The majority of endothelial cells, identified by CD31 (green), in the heart of PD-L1^{-/-};^{MRL-+/+} BM recipients expressed PD-L1 (red) as shown in the merged images (yellow) (Fig 7A, bottom left panels). However, some PD-L1⁺ cells are not CD31⁺ (red only), and most likely correspond to myocytes that are surrounded by infiltrating PD-L1^{-/-} leukocytes (pale staining areas). Similarly, we detected a dramatic up-regulation of PD-L1 throughout the lung on endothelial cells in PD-L1^{-/-};^{MRL-+/+} BM recipients (data not shown). This striking induction of PD-L1 expression on the endothelium in the heart and lung with inflammation suggests that PD-L1 expression on parenchymal cells may play a role in limiting tissue damage once tolerance is broken.

Discussion

Our studies reveal a critical role for PD-L1 in controlling autoimmune heart and lung disease. PD-L1^{-/-};^{MRL-Fas^{lpr}} mice spontaneously develop a fulminant, fatal autoimmune myocarditis that resembles human autoimmune myocarditis (33). This is a dramatic finding since MRL-Fas^{lpr} mice do not have overt heart disease and typically succumb to a kidney illness. Perhaps, even more remarkable is the emergence of an aggressive autoimmune disease in PD-L1^{-/-};^{MRL-+/+} mice (Fas-intact), since WT;^{MRL-+/+} mice typically develop a more latent disease than WT;^{MRL-Fas^{lpr}} mice. As PD-L1^{-/-} mice on other backgrounds (B6 and BALB/c) are healthy (26) and PD-L1^{-/-};^{B6} mice require the Fas^{lpr} mutation for consistent glomerulonephritis (21), this finding indicates that MRL background genes are central to autoimmune disease. In addition, our results highlight a dominant role for PD-L1 in protecting the heart and lungs in WT;^{MRL-Fas^{lpr}} mice. Taken together, these data emphasize that the interaction of PD-L1 with MRL background genes dictates the phenotype of autoimmune disease.

The broad distribution of PD-L1 expression on hematopoietic and parenchymal cells suggests one or both cell types may be central to limiting autoimmune disease during multiple phases of the immune response. The transfer of autoimmune myocarditis with PD-L1^{-/-};^{MRL-+/+} BM suggests that disease is initiated by PD-L1^{-/-} leukocytes. In PD-L1^{-/-};^{MRL} mice the majority of infiltrates in the heart and lung are M ϕ . This is in keeping with the predominance of this subset in the kidney, liver, spleen, and skin during inflammation in MRL-Fas^{lpr} mice (34, 35). Transgenic over-expression of MCP-1 by myocardial tissue indicates that recruitment of M ϕ is sufficient to induce myocarditis (36). However, there are substantial numbers of T cells in the heart and lung of PD-L1^{-/-};^{MRL} mice and there is a central role for T cells in other spontaneous models of myocarditis (37-39). While CD8⁺ T cells initiate disease, CD4⁺ T are the primary effectors (39). Thus, it is likely that each of these subsets contributes to the pathogenesis of myocarditis in PD-L1^{-/-};^{MRL} mice. Further experiments are needed to decipher the specific role of PD-L1 expression by M ϕ , and other leukocytic subsets in the induction and progression of myocarditis in MRL mice.

Although we transferred disease into WT;^{MRL-+/+} mice with PD-L1^{-/-};^{MRL-+/+} BM cells; myocarditis was more severe in PD-L1^{-/-};^{MRL-+/+} mice, which lack PD-L1 expression on hematopoietic and parenchymal cells. Consistent with this finding, PD-L1 expression is dramatically up-regulated in the heart and lung, primarily by endothelial cells, after the induction of inflammation by the transfer of PD-L1^{-/-};^{MRL-+/+} BM cells. Interestingly, PD-L1 expression on non-hematopoietic is primarily important for prevention of diabetes in NOD mice (26), while PD-L1 expression by hematopoietic cells primarily limits inflammation in an experimental model of autoimmune kidney disease (17). Thus, PD-L1 expression by different

cell types is dominant in specific diseases and tissues. By comparison, PD-L1 expression on both host and donor cells is required to limit cardiac (40) or corneal allograft rejection (41). In these models, it is likely that PD-L1 expression on host APCs during the priming phase prevents the induction of alloreactive cells, while PD-L1 expression on donor parenchymal cells limits leukocytic infiltration once the immune response is initiated. Based on these findings, we hypothesize that there is a role for PD-L1 expression on parenchymal cells in limiting myocarditis and pneumonitis once disease is initiated in MRL mice. While we attempted to test this concept directly by transferring PD-L1^{-/-};MRL^{+/+} BM into WT;MRL^{+/+} and PD-L1^{-/-};MRL^{+/+} hosts; the rapidity of disease in PD-L1^{-/-};MRL^{+/+} mice compromised the interpretation of these results. Likewise, it would be interesting to examine whether WT;MRL^{+/+} BM prevents disease in PD-L1^{-/-};MRL^{+/+} mice, but again the rapid onset of disease in PD-L1^{-/-};MRL^{+/+} mice hamper these studies.

To determine whether heart-specific autoAbs were involved in heart disease in PD-L1^{-/-};MRL^{+/+} mice, we probed for anti-cardiac myosin and anti-cardiac troponin I autoAbs. While we did not detect these autoAbs at early time points (2 wk and 1 mo), we did detect high titers of cardiac-specific autoAbs once myocarditis was established (2 mo). Anti-cardiac myosin autoAbs are prevalent during myocarditis and induce myocarditis in susceptible mouse strains (42-44). In addition, immunization with cardiac troponin I induces myocarditis (45). Therefore, in four separate experiments, we transferred serum from moribund PD-L1^{-/-};MRL^{+/+} mice into WT;MRL^{-/-}*FasIpr* (n=10) and WT;MRL^{+/+} (n=7) mice and examined hearts 10-14 days after transfer for myocarditis. Serum from PD-L1^{-/-};MRL^{+/+} did not induce any signs of myocarditis in WT;MRL^{+/+} mice. While we appreciate there are numerous variables (timing, amount of serum, etc) that affect the outcome of this experiment, these findings suggest it is unlikely these autoAbs are central to initiating myocarditis in PD-L1^{-/-};MRL^{+/+} mice. These results are consistent with our finding that heart-specific autoAbs in the serum and C3 deposits in the tissue are not detectable until late in the disease process. However, it remains possible that IgG deposits in the heart may contribute to myocarditis in PD-L1^{-/-};MRL^{+/+} mice via complement independent mechanisms (Fc receptor engagement, cell surface receptor engagement, etc). In any case, our findings differ from PD-1^{-/-};BALB/c mice that develop dilated cardiomyopathy (32), which has been attributed to cardiac-specific autoAbs (31). However, as PD-L1/PD-L2^{-/-};BALB/c mice do not develop heart disease or have an increase in the rate of mortality, a role for the PD-1/PD-L pathway in the emergence of cardiomyopathy in the PD-1^{-/-};BALB/c mice is questionable.

In summary, PD-L1 is a critical checkpoint that protects the heart and lung in the autoimmune MRL mouse strains. Our findings are consistent with accumulating data, which indicate that disruption of PD-1/PD-L1 pathway accelerates autoimmune disease. In addition, we now report that the phenotype of autoimmune disease is dramatically altered in PD-L1^{-/-};MRL^{+/+} mice. Similar to MRL mice, human autoimmune diseases often have multiple manifestations; and the differences in patients' symptoms may be attributed to polymorphisms in specific genes. Interestingly, polymorphisms in the PD-1 gene are associated with several autoimmune diseases including: lupus, type 1 diabetes, rheumatoid arthritis, Grave's disease, and multiple sclerosis (20,46). As a subset of human lupus patients develops heart and lung disease, including myocarditis and pneumonitis, it is intriguing to speculate that polymorphisms in PD-1 and/or PD-L1 may regulate lupus in patients.

Acknowledgements

We would like to thank Dr. Andrew Lichtman (Brigham and Women's Hospital, Boston, MA) for insightful discussions, Mary Keir and George Stavrakis for technical advice and assistance, Rodrick Bronson for assistance in evaluating pathology, and Dr. Gordon Freeman (Dana Farber Cancer Institute, Boston, MA) for providing the anti-PD-1 Ab.

Abbreviations used in this paper

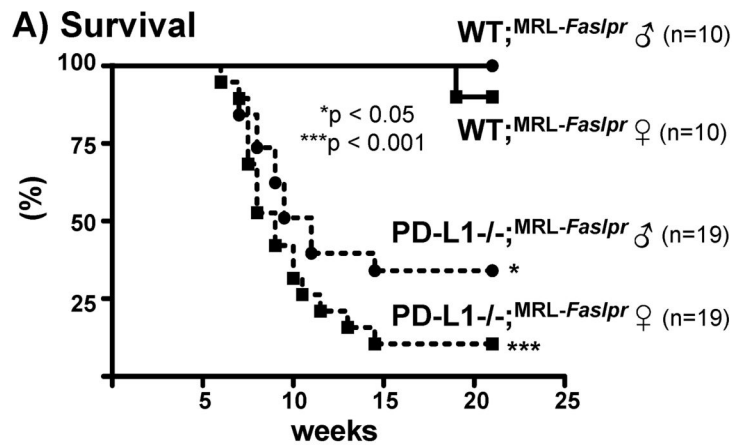
MRL-*Fas*^{lpr}, MRL/MpJ-*Fas*^{lpr}; MRL-+/, MRL/MpJ; C57BL/6, B6; PD-1, programmed-death 1; PD-L1, PD-1 ligand; PD-L2, PD-1 ligand 2; Mø, macrophage; WT, wild type; autoAbs, autoantibodies; BM, bone marrow.

References

1. Theofilopoulos AN, Dixon FJ. Etiopathogenesis of murine SLE. *Immunol. Rev* 1981;55:179–216. [PubMed: 6165672]
2. Kelley VE, Roths JB. Interaction of mutant *lpr* gene with background strain influences renal disease. *Clin. Immunol. Immunopathol* 1985;37:220–229. [PubMed: 4042431]
3. Moyer CF, Strandberg JD, Reinisch CL. Systemic mononuclear-cell vasculitis in MRL/Mp-*lpr/lpr* mice. A histologic and immunocytochemical analysis. *Am. J. Pathol* 1987;127:229–242. [PubMed: 3107393]
4. Andrews BS, Eisenberg RA, Theofilopoulos AN, Izui S, Wilson CB, McConahey PJ, Murphy ED, Roths JB, Dixon FJ. Spontaneous murine lupus-like syndromes. Clinical and immunopathological manifestations in several strains. *J. Exp. Med* 1978;148:1198–1215. [PubMed: 309911]
5. Matsuzawa A, Moriyama T, Kaneko T, Tanaka M, Kimura M, Ikeda H, Katagiri T. A new allele of the *lpr* locus, *lprcg*, that complements the *gld* gene in induction of lymphadenopathy in the mouse. *J. Exp. Med* 1990;171:519–531. [PubMed: 2406366]
6. Watanabe-Fukunaga R, Brannan CI, Copeland NG, Jenkins NA, Nagata S. Lymphoproliferation disorder in mice explained by defects in Fas antigen that mediates apoptosis. *Nature* 1992;356:314–317. [PubMed: 1372394]
7. Peng SL, Madaio MP, Hughes DP, Crispe IN, Owen MJ, Wen L, Hayday AC, Craft J. Murine lupus in the absence of alpha beta T cells. *J. Immunol* 1996;156:4041–4049. [PubMed: 8621947]
8. Christianson GJ, Blankenburg RL, Duffy TM, Panka D, Roths JB, Marshak-Rothstein A, Roopenian DC. beta2-microglobulin dependence of the lupus-like autoimmune syndrome of MRL-*lpr* mice. *J. Immunol* 1996;156:4932–4939. [PubMed: 8648144]
9. Chesnutt MS, Finck BK, Killeen N, Connolly MK, Goodman H, Wofsy D. Enhanced lymphoproliferation and diminished autoimmunity in CD4-deficient MRL/*lpr* mice. *Clin. Immunol. Immunopathol* 1998;87:23–32. [PubMed: 9576007]
10. Lenda DM, Stanley ER, Kelley VR. Negative role of colony-stimulating factor-1 in macrophage, T cell, and B cell mediated autoimmune disease in MRL-*Fas(lpr)* mice. *J. Immunol* 2004;173:4744–4754. [PubMed: 15383612]
11. Chan OT, Madaio MP, Shlomchik MJ. The central and multiple roles of B cells in lupus pathogenesis. *Immunol. Rev* 1999;169:107–121. [PubMed: 10450512]
12. Hewicker M, Trautwein G. Glomerular lesions in MRL mice. A light and immunofluorescence microscopic study. *Zentralbl. Veterinarmed. B* 1986;33:727–739. [PubMed: 3551406]
13. Watson ML, Rao JK, Gilkeson GS, Ruiz P, Eicher EM, Pisetsky DS, Matsuzawa A, Rochelle JM, Seldin MF. Genetic analysis of MRL-*lpr* mice: relationship of the Fas apoptosis gene to disease manifestations and renal disease-modifying loci. *J. Exp. Med* 1992;176:1645–1656. [PubMed: 1460423]
14. Vidal S, Kono DH, Theofilopoulos AN. Loci predisposing to autoimmunity in MRL-*Fas lpr* and C57BL/6-*Faslpr* mice. *J. Clin. Invest* 1998;101:696–702. [PubMed: 9449705]
15. Kinoshita K, Tesch G, Schwarting A, Maron R, Sharpe AH, Kelley VR. Costimulation by B7-1 and B7-2 is required for autoimmune disease in MRL-*Faslpr* mice. *J. Immunol* 2000;164:6046–6056. [PubMed: 10820290]
16. Agata Y, Kawasaki A, Nishimura H, Ishida Y, Tsubata T, Yagita H, Honjo T. Expression of the PD-1 antigen on the surface of stimulated mouse T and B lymphocytes. *Int. Immunol* 1996;8:765–772. [PubMed: 8671665]
17. Menke J, Lucas JA, Zeller GC, Keir ME, Huang XR, Tsuboi N, Mayadas TN, Lan HY, Sharpe AH, Kelley VR. Programmed Death 1 Ligand (PD-L) 1 and PD-L2 Limit Autoimmune Kidney Disease: Distinct Roles. *J. Immunol* 2007;179:7466–7477. [PubMed: 18025191]

18. Gotsman I, Grabie N, Dacosta R, Sukhova G, Sharpe A, Lichtman AH. Proatherogenic immune responses are regulated by the PD-1/PD-L pathway in mice. *J. Clin. Invest* 2007;117:2974–2982. [PubMed: 17853943]
19. Sharpe AH, Wherry EJ, Ahmed R, Freeman GJ. The function of programmed cell death 1 and its ligands in regulating autoimmunity and infection. *Nat. Immunol* 2007;8:239–245. [PubMed: 17304234]
20. Keir ME, Butte MJ, Freeman GJ, Sharpe AH. PD-1 and Its Ligands in Tolerance and Immunity. *Annu. Rev. Immunol.* 2008
21. Nishimura H, Nose M, Hiai H, Minato N, Honjo T. Development of lupus-like autoimmune diseases by disruption of the PD-1 gene encoding an ITIM motif-carrying immunoreceptor. *Immunity* 1999;11:141–151. [PubMed: 10485649]
22. Latchman YE, Liang SC, Wu Y, Chernova T, Sobel RA, Klemm M, Kuchroo VK, Freeman GJ, Sharpe AH. PD-L1-deficient mice show that PD-L1 on T cells, antigen-presenting cells, and host tissues negatively regulates T cells. *Proc. Natl. Acad. Sci. U S A* 2004;101:10691–10696. [PubMed: 15249675]
23. Watson ML, Rao JK, Gilkeson GS, Ruiz P, Eicher EM, Pisetsky DS, Matsuzawa A, Rochelle JM, Seldin MF. Genetic analysis of MRL-lpr mice: relationship of the Fas apoptosis gene to disease manifestations and renal disease-modifying loci. *J Exp Med* 1992;176:1645–1656. [PubMed: 1460423]
24. Taqueti VR, Grabie N, Colvin R, Pang H, Jarolim P, Luster AD, Glimcher LH, Lichtman AH. T-bet controls pathogenicity of CTLs in the heart by separable effects on migration and effector activity. *J. Immunol* 2006;177:5890–5901. [PubMed: 17056513]
25. O'Connor KC, Nguyen K, Stollar BD. Recognition of DNA by VH and Fv domains of an IgG anti-poly(dC) antibody with a singly mutated VH domain. *J Mol Recognit* 2001;14:18–28. [PubMed: 11180559]
26. Keir ME, Liang SC, Guleria I, Latchman YE, Qipo A, Albacker LA, Koulmanda M, Freeman GJ, Sayegh MH, Sharpe AH. Tissue expression of PD-L1 mediates peripheral T cell tolerance. *J. Exp. Med* 2006;203:883–895. [PubMed: 16606670]
27. Njoroge JM, Mitchell LB, Centola M, Kastner D, Raffeld M, Miller JL. Characterization of viable autofluorescent macrophages among cultured peripheral blood mononuclear cells. *Cytometry* 2001;44:38–44. [PubMed: 11309807]
28. Lund FE. Cytokine-producing B lymphocytes-key regulators of immunity. *Curr Opin Immunol.* 2008
29. Li Y, Heuser JS, Cunningham LC, Kosanke SD, Cunningham MW. Mimicry and antibody-mediated cell signaling in autoimmune myocarditis. *J. Immunol* 2006;177:8234–8240. [PubMed: 17114501]
30. Cunningham MW. T cell mimicry in inflammatory heart disease. *Mol. Immunol* 2004;40:1121–1127. [PubMed: 15036918]
31. Okazaki T, Tanaka Y, Nishio R, Mitsuiye T, Mizoguchi A, Wang J, Ishida M, Hiai H, Matsumori A, Minato N, Honjo T. Autoantibodies against cardiac troponin I are responsible for dilated cardiomyopathy in PD-1-deficient mice. *Nat. Med* 2003;9:1477–1483. [PubMed: 14595408]
32. Nishimura H, Okazaki T, Tanaka Y, Nakatani K, Hara M, Matsumori A, Sasayama S, Mizoguchi A, Hiai H, Minato N, Honjo T. Autoimmune dilated cardiomyopathy in PD-1 receptor-deficient mice. *Science* 2001;291:319–322. [PubMed: 11209085]
33. Schoen, FJ. The heart.. In: Kumar, V.; Fausto, N.; Abbas, A., editors. *Robbins/Cotran Pathologic Basis of Disease*. 7th ed.. W.B. Saunders; Philadelphia, PA: 2004. p. 555-618.
34. Bloom RD, Florquin S, Singer GG, Brennan DC, Kelley VR. Colony stimulating factor-1 in the induction of lupus nephritis. *Kidney Int* 1993;43:1000–1009. [PubMed: 8510378]
35. Yui MA, Brissette WH, Brennan DC, Wuthrich RP, Rubin-Kelley VE. Increased macrophage colony-stimulating factor in neonatal and adult autoimmune MRL-lpr mice. *Am. J. Pathol* 1991;139:255–261. [PubMed: 1867317]
36. Kolattukudy PE, Quach T, Bergese S, Breckenridge S, Hensley J, Altschuld R, Gordillo G, Klenotic S, Orosz C, Parker-Thornburg J. Myocarditis induced by targeted expression of the MCP-1 gene in murine cardiac muscle. *Am. J. Pathol* 1998;152:101–111. [PubMed: 9422528]
37. Elliott JF, Liu J, Yuan ZN, Bautista-Lopez N, Wallbank SL, Suzuki K, Rayner D, Nation P, Robertson MA, Liu G, Kavanagh KM. Autoimmune cardiomyopathy and heart block develop spontaneously

- in HLA-DQ8 transgenic IAbeta knockout NOD mice. *Proc. Natl. Acad. Sci. U S A* 2003;100:13447–13452. [PubMed: 14570980]
38. Taylor JA, Havari E, McInerney MF, Bronson R, Wucherpfennig KW, Lipes MA. A spontaneous model for autoimmune myocarditis using the human MHC molecule HLA-DQ8. *J. Immunol* 2004;172:2651–2658. [PubMed: 14764740]
 39. Hayward SL, Bautista-Lopez N, Suzuki K, Atrazhev A, Dickie P, Elliott JF. CD4 T cells play major effector role and CD8 T cells initiating role in spontaneous autoimmune myocarditis of HLA-DQ8 transgenic IAb knockout nonobese diabetic mice. *J. Immunol* 2006;176:7715–7725. [PubMed: 16751419]
 40. Tanaka K, Albin MJ, Yuan X, Yamaura K, Habicht A, Murayama T, Grimm M, Waaga AM, Ueno T, Padera RF, Yagita H, Azuma M, Shin T, Blazar BR, Rothstein DM, Sayegh MH, Najafian N. PDL1 is required for peripheral transplantation tolerance and protection from chronic allograft rejection. *J. Immunol* 2007;179:5204–5210. [PubMed: 17911605]
 41. Shen L, Jin Y, Freeman GJ, Sharpe AH, Dana MR. The function of donor versus recipient programmed death-ligand 1 in corneal allograft survival. *J. Immunol* 2007;179:3672–3679. [PubMed: 17785803]
 42. Liao L, Sindhvani R, Rojkind M, Factor S, Leinwand L, Diamond B. Antibody-mediated autoimmune myocarditis depends on genetically determined target organ sensitivity. *J. Exp. Med* 1995;181:1123–1131. [PubMed: 7869033]
 43. Kuan AP, Chamberlain W, Malkiel S, Lieu HD, Factor SM, Diamond B, Kotzin BL. Genetic control of autoimmune myocarditis mediated by myosin-specific antibodies. *Immunogenetics* 1999;49:79–85. [PubMed: 9887344]
 44. Kuan AP, Zuckier L, Liao L, Factor SM, Diamond B. Immunoglobulin isotype determines pathogenicity in antibody-mediated myocarditis in naive mice. *Circ. Res* 2000;86:281–285. [PubMed: 10679479]
 45. Goser S, Andrassy M, Buss SJ, Leuschner F, Volz CH, Ottl R, Zittrich S, Blaudeck N, Hardt SE, Pfitzer G, Rose NR, Katus HA, Kaya Z. Cardiac troponin I but not cardiac troponin T induces severe autoimmune inflammation in the myocardium. *Circulation* 2006;114:1693–1702. [PubMed: 17015788]
 46. Okazaki T, Honjo T. PD-1 and PD-1 ligands: from discovery to clinical application. *Int. Immunol* 2007;19:813–824. [PubMed: 17606980]



B) Hearts

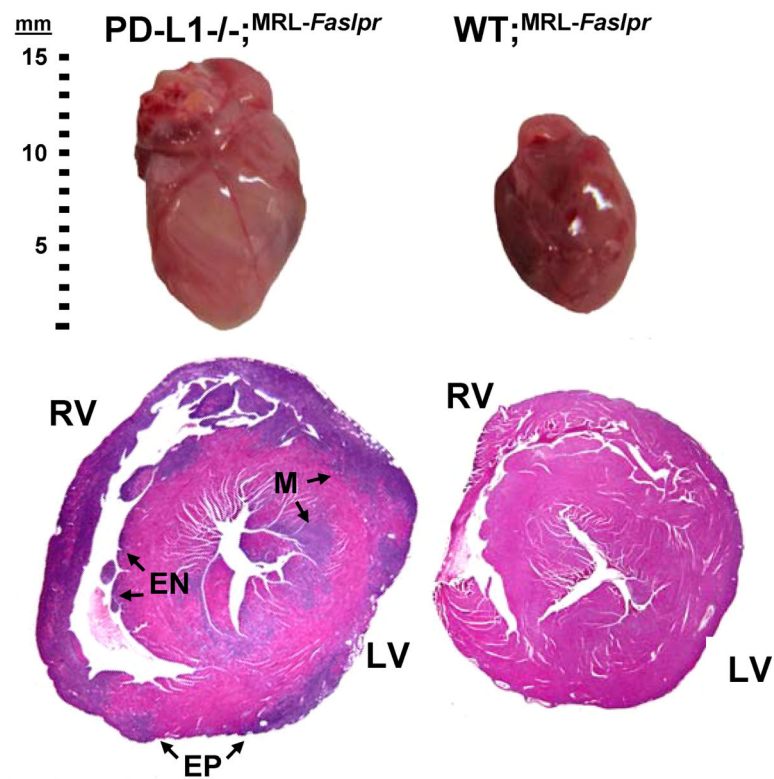


Figure 1. PD-L1^{-/-};MRL-*Faslpr* mice die more rapidly than WT;MRL-*Faslpr* mice with enlarged hearts

A) Kaplan-Meier survival curves of PD-L1^{-/-};MRL-*Faslpr* and WT;MRL-*Faslpr* littermates. B) Photograph of whole hearts (top) and lateral H&E stained heart sections (2X) from moribund PD-L1^{-/-};MRL-*Faslpr* (left) and WT;MRL-*Faslpr* mice (right) (2 mo). Involvement of the right and left ventricles, (RV and LV, respectively) as well as the epicardium (EP), endocardium (EN), and myocardium (M) is indicated. Note the transmural involvement of nearly the entire right ventricle.

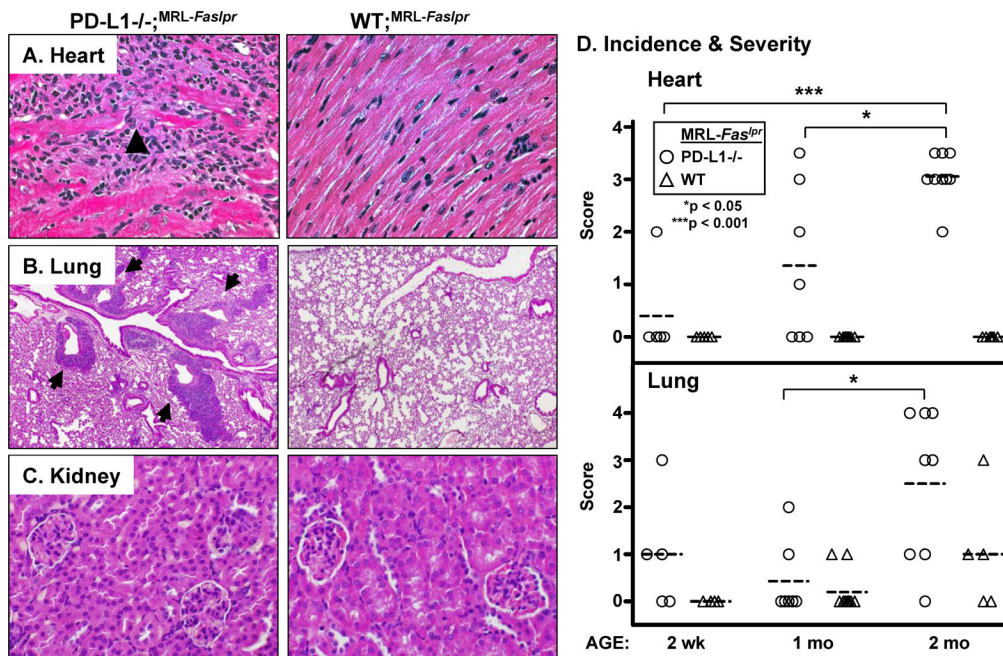


Figure 2. PD-L1^{-/-};MRL-Faslpr mice spontaneously develop severe myocarditis and pneumonitis, but not renal disease

Photomicrographs of A) heart ventricle (40X) B) lung (10X), and C) kidney sections (40X) from PD-L1^{-/-};MRL-Faslpr and WT;MRL-Faslpr mice (2 mo). A) Arrowheads indicate areas of myocyte damage. B) Arrows (left panel) indicate pulmonary vessels surrounded by mononuclear cells. H&E stained sections. D) Temporal analysis of myocarditis (top) and pneumonitis (bottom) in PD-L1^{-/-};MRL-Faslpr and WT;MRL-Faslpr mice at 2 wk, 1, and 2 mo of age (n = 4–10 mice/group) using separate scoring systems (0–4). Means are indicated by dashed line.

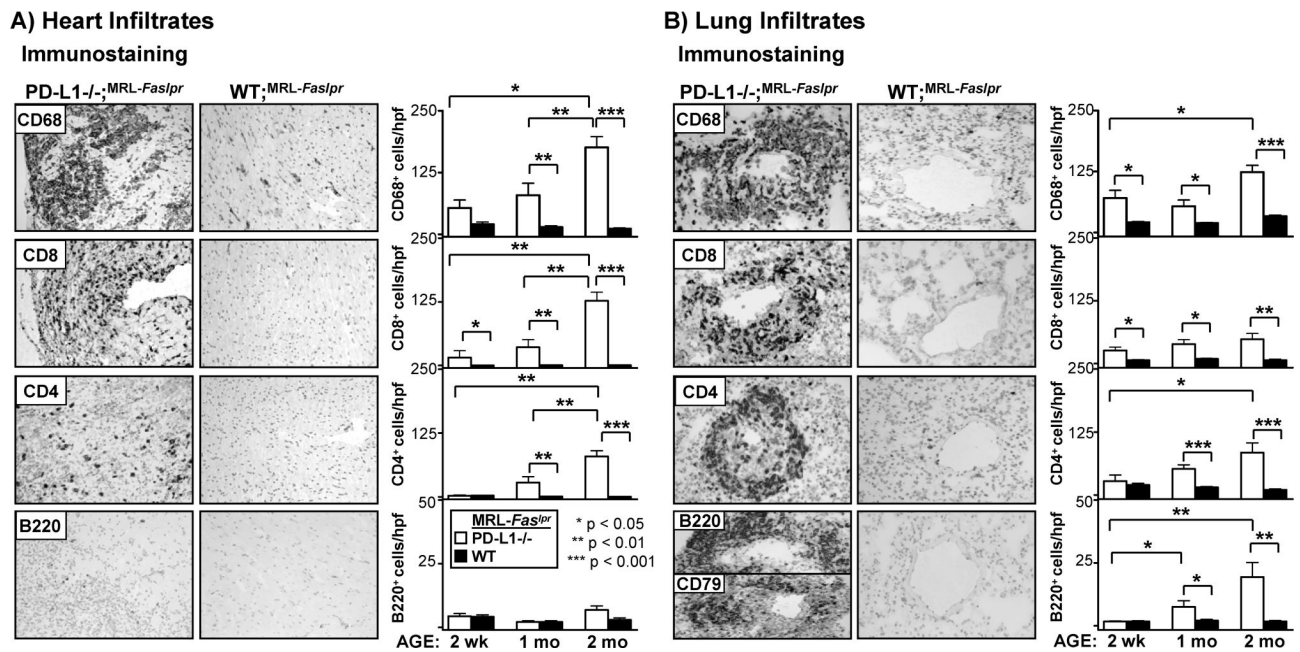


Figure 3. M ϕ and T cell infiltrates are increased in the heart and lung of PD-L1^{-/-};MRL-Faslpr mice

The presence of M ϕ , T cells (CD4⁺ and CD8⁺), and B220⁺ cells in the heart and lung of PD-L1^{-/-};MRL-Faslpr and WT;MRL-Faslpr mice was evaluated at 2wk, 1, and 2 mo of age by immunohistochemistry. Representative photomicrographs (20X) of A) heart and B) lung sections from PD-L1^{-/-};MRL-Faslpr and WT;MRL-Faslpr mice (2 mo). Lung sections were stained with CD79 to distinguish B cells and DN T cells (bottom left panel). Heart infiltrates were quantitated by counting 10 high power fields (hpf)/section and perivascular lung infiltrates were quantitated by counting 10 vessels/section. Data are mean \pm SEM.

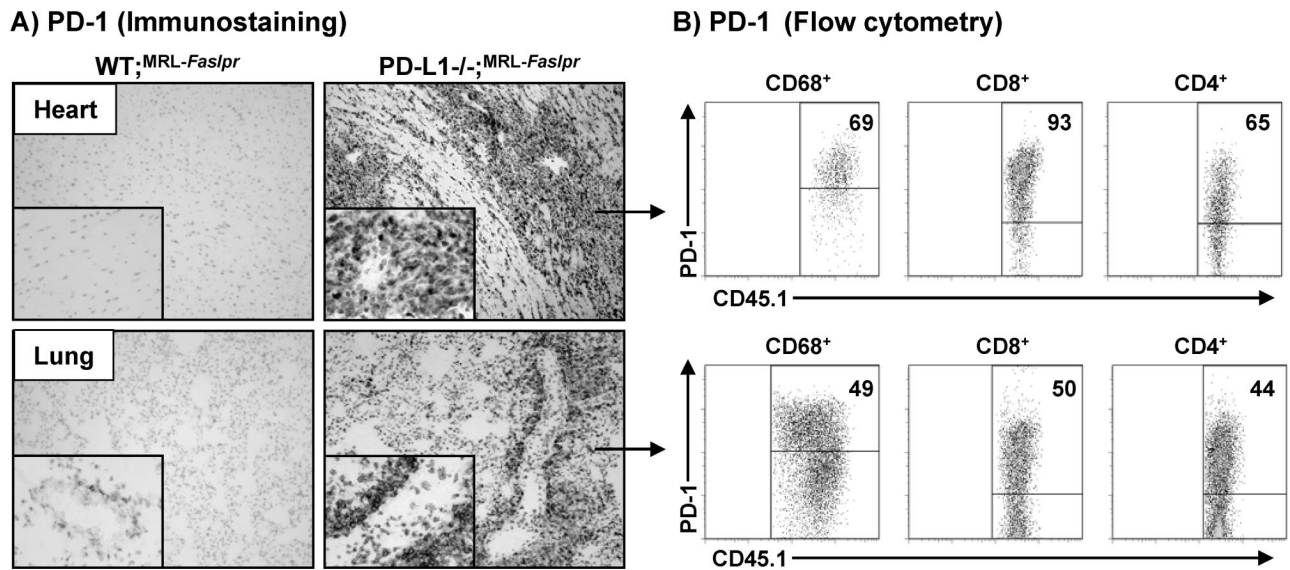


Figure 4. PD-1 expression is increased in the heart and lung of PD-L1^{-/-};^{MRL-FasIpr} mice
 PD-1 expression was evaluated in the heart and lung of WT;^{MRL-FasIpr} and PD-L1^{-/-};^{MRL-FasIpr} mice (2 mo) by immunohistochemistry (frozen sections) and flow cytometry. A) Representative photomicrographs (10X, with 40X inset) of heart (top) and lung (bottom). B) Flow cytometric analysis of PD-1 expression in the heart and lung of PD-L1^{-/-};^{MRL-FasIpr} mice (2 mo). Heart (top) and lung (bottom) single cell suspensions were gated on CD68⁺, CD8⁺, or CD4⁺ cells. Representative flow cytometry plots with the percentage of PD-L1⁺CD45.1⁺ cells within these populations are shown.

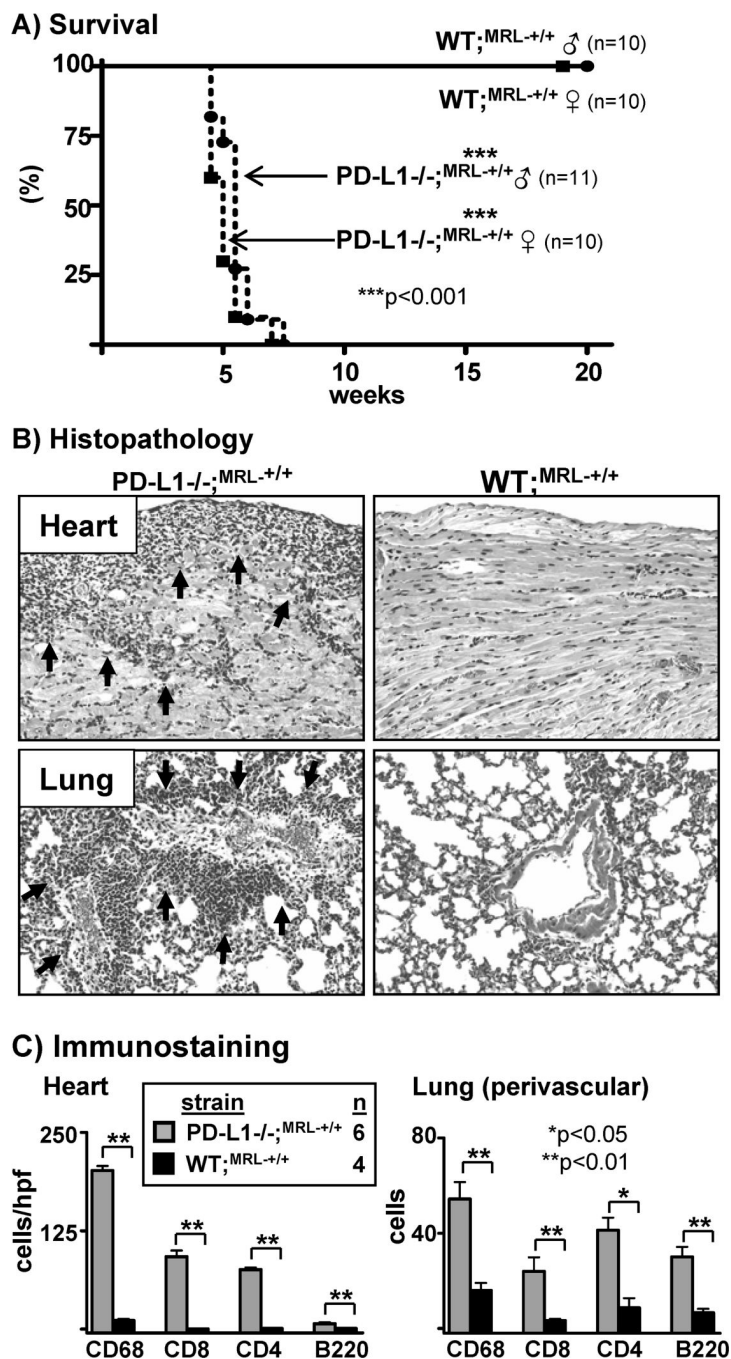


Figure 5. Myocarditis and pneumonitis in PD-L1^{-/-};MRL^{-/-}Fas^{lpr} mice is not dependent on the Fas^{lpr} mutation

A) Kaplan-Meier survival curves of PD-L1^{-/-};MRL^{+/+} males and females. B) Heart and lung sections (20X) from moribund PD-L1^{-/-};MRL^{+/+} and age-matched WT;MRL^{+/+} mice. Arrows indicate areas of mononuclear cell infiltration. C) Heart and lung infiltrates were assessed in moribund PD-L1^{-/-};MRL^{+/+} and age-matched WT;MRL^{+/+} mice as in Fig 4.

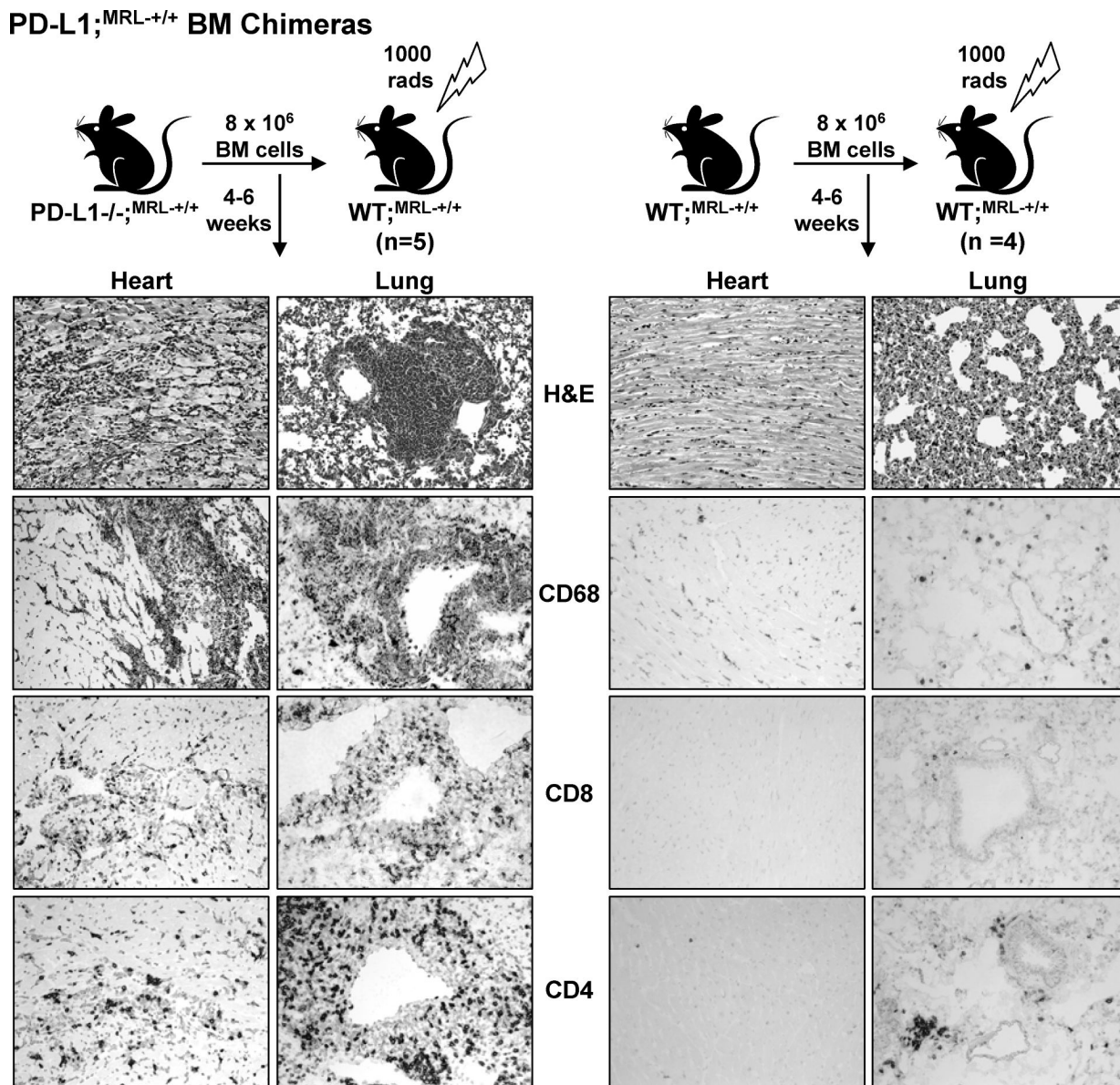


Figure 6. Myocarditis and pneumonitis develop when PD-L1^{-/-};MRL^{+/+} BM is transferred into WT;MRL^{+/+} mice

BM cells (8×10^6) from PD-L1^{-/-};MRL^{+/+} and WT;MRL^{+/+} mice were injected (i.v.) into lethally irradiated (1000 rad) WT;MRL^{+/+} mice. Myocarditis and pneumonitis was evaluated by histopathology (H&E) and immunostaining for the presence of CD68⁺, CD8⁺, and CD4⁺ cells. Representative photomicrographs are of heart and lung sections (20X).

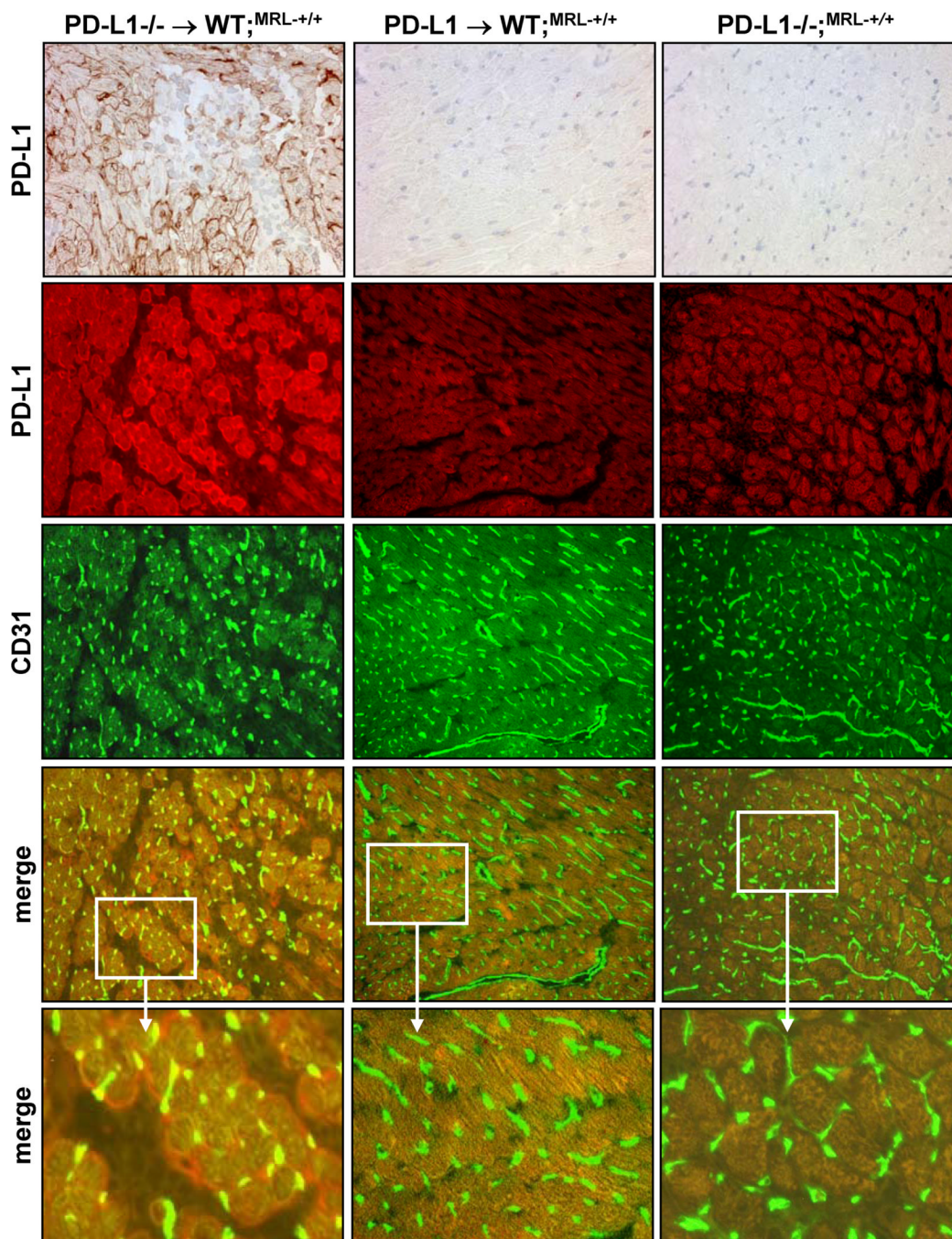


Figure 7. PD-L1 expression is up-regulated on endothelial cells in the heart and lung when inflammation is induced in WT;^{MRL-+/+} mice

PD-L1 expression was analyzed on frozen heart sections from irradiated WT;^{MRL-+/+} mice reconstituted with PD-L1^{-/-};^{MRL-+/+} BM (left panels) or WT;^{MRL-+/+} BM (middle panels), or PD-L1^{-/-};^{MRL} mice (right panels) by immunohistochemistry (top row) and immunofluorescence (second row, red). Endothelial cells are detected by CD31 expression (third row, green). Co-staining for CD31 and PD-L1 are in merged images (fourth and fifth rows, yellow). Representative photomicrographs (20X), except bottom row, which is an enlarged area (3X) of 20X image marked by white box.